

Ethane measurement by Picarro CRDS G2201-i in laboratory and field conditions: potential and limitations

Sara M. Defratyka¹, Jean-Daniel Paris¹, Camille Yver-Kwok¹, Daniel Loeb^{1, *}, James France^{2, 3}, Jon Helmore⁴, Nigel Yarrow⁴, Valérie Gros¹, Philippe Bousquet¹

5 1 Laboratoire des Sciences du Climat et de l'Environnement (LSCE-IPSL) CEA-CNRS-UVSQ Université Paris Saclay, Gif-sur-Yvette, 91191, France

2 Royal Holloway University of London, Egham, TW20 0EX, United Kingdom

3 British Antarctic Survey, Natural Environment Research Council, Cambridge CB3 0ET, UK

4 National Physical Laboratory (NPL), Hampton Road, Teddington, TW11 0LW Middlesex, UK

10 *Now at Université Paris-Saclay, Orsay 91400

Correspondence to: Sara M. Defratyka (sara.defratyka@lsce.ipsl.fr)

Abstract. Atmospheric ethane can be used as a tracer to distinguish methane sources, both at local and global scale. Currently, ethane can be measured in the field using flasks or in-situ analyzers. In our study, we characterized the CRDS Picarro G2201-i instrument, originally designed to measure isotopic CH₄ and CO₂, for measurements of ethane to methane ratio in mobile measurement scenarios, near-sources, and under field conditions. We evaluated the limitations and potential of using the CRDS G2201-i to measure the ethane to methane ratio, thus extending the instrument application to simultaneously measure two methane source proxies in the field: carbon isotopic ratio and the ethane to methane ratio. First, laboratory tests were run to characterize the instrument in stationary conditions. Subsequently, the instrument performance was tested in field conditions, as part of a controlled release experiment. Finally, the instrument was tested during mobile measurements focused on gas compressor stations. The results from the field were afterwards compared with the results obtained from instruments specifically designed for ethane measurements. Our study shows the potential of using the CRDS G2201-i instrument in a mobile configuration to determine the ethane to methane ratio in methane plumes under measurement conditions with an ethane uncertainty of 50 ppb. Assuming typical ethane to methane ratios ranging between 0 and 0.1 ppb ppb⁻¹, we conclude that the instrument can accurately estimate the “true” ethane to methane ratio within 1-sigma uncertainty when CH₄ enhancements are at least 1 ppm, as can be found in the vicinity of strongly emitting sites such as natural gas compressor stations and roadside gas pipeline leaks.

1. Introduction

Methane (CH₄) is the second most potent anthropogenic greenhouse gas almost three times the with an average atmospheric mixing ratio reaching up to 1892 ppb on the global scale in November 2020 (Dlugokencky, 2021), almost three times more than during the pre-industrial era. Anthropogenic methane emissions amount to more than half of the total input of methane to the atmosphere and include a range of sources such as landfills wastewater treatment plants, agriculture, coal, oil, and natural

gas industries (IPCC, 2018; Turner et al., 2019; Saunois et al., 2020). Large uncertainties remain in the quantification of these sources' magnitudes and locations (Saunois et al., 2016). The variety of methane sources and their geographical overlap increase the difficulty of closing the present methane budget from global to local scale.

35 Methane sources often co-emit a specific mixture of other gases that can be used as tracers to identify them. For instance, ethane (C_2H_6) is associated with thermogenic methane and is therefore co-emitted during extraction of coal, oil and natural gas as well as transportation of the latter (e.g., Aydin et al., 2011; Hausmann et al., 2016; Helmig et al., 2016; Schwietzke et al., 2014; Sherwood et al., 2017; Simpson et al., 2012). Typically, the C_2H_6 mixing ratio in the clean continental atmosphere ranges between 0.5 – 2 ppb but it can reach up to 1000 ppb in the vicinity of methane and ethane emitters, such as gas production
40 facilities (Simpson et al. 2012, Rella et al. 2017). In the case of the natural gas industry, a range of values for ethane to methane ($C_2H_6:CH_4$) are observed depending on the geological reservoir from which the gas has been extracted and on its eventual processing. The reported ratios (calculated as molar ratio when based on atmospheric measurements) depend on the type of production facilities and hydrocarbon reservoirs: From 0.01 to 0.06 for gas leaks and gas compressors (Lopez et al., 2017; Lowry et al., 2020; Yacovitch et al., 2014), or higher than 0.3 for processed natural gas liquids (Kort et al., 2016; Yacovitch et al., 2014). Different ratios are also observed in the case of dry gas (0.01-0.06) and wet gas (>0.06). Regarding offshore oil and gas platforms, $C_2H_6:CH_4$ typically are around 0.05, but ratios of 0.002 and 0.17 have been observed (Yacovitch et al., 2020). Recent studies (Lan et al. 2019; Turner et al., 2019; Yacovitch et al., 2020) showed varying $C_2H_6:CH_4$ ratios for different
45 facilities, even at the local scale. Lan et al. (2019) showed an increase of $C_2H_6:CH_4$ on Oil and Natural Gas observation sites in the National Oceanic and Atmospheric Administration Global Greenhouse Gas Reference Network (GGRN) over the course
50 of the respective measurement period. On the contrary, biogenic sources such as landfills and cattle farms show either zero or only very small values (<0.002) of $C_2H_6:CH_4$ ratios (Assan et al., 2017; Yacovitch et al., 2014).

At the local scale, observing changes in $C_2H_6:CH_4$ provides additional information about specific methane sources, especially in areas with multiple CH_4 enhancements from unknown origins (Assan et al., 2017; Lopez et al., 2017; Lowry et al., 2020; Yacovitch et al., 2014, 2020). The currently available techniques, such as gas chromatography with a flame ionization detector
55 (GC-FID) and Fourier-transform infrared spectroscopy (FTIR) provide long-term or short-term (e.g. hourly timescale) measurements of ethane and other components in stationary conditions (Bourtsoukidis et al., 2019; Gros et al., 2011; Hausmann et al., 2016; McKain et al., 2015; Yang et al., 2005; Paris et al., 2021). Laser-based instruments, such as the Los Gatos Research (LGR) Ultraportable Methane:Ethane Analyzer (UMEA), based on a cavity-enhanced absorption technique, the Picarro Cavity ring down spectroscopy (CRDS) analyzers (Rella et al. 2015) and the tunable infrared laser direct absorption
60 spectroscopy (TILDAS) analyzer (Smith et al., 2015; Yacovitch et al., 2014) make it possible to measure ethane at high frequency and on a mobile platform. Here, building on previous studies with CRDS instruments, we specify the possibilities and limitations of measuring C_2H_6 using the CRDS G2201-i, in the vicinity of a methane sources. The CRDS G2201-i is originally designed to measure $^{12}CO_2$, $^{13}CO_2$, $^{12}CH_4$, $^{13}CH_4$ and H_2O and records C_2H_6 only as an internal way to correct $^{13}CH_4$, thus observed the C_2H_6 mixing ratio must be corrected and calibrated.

65 Previous studies already showed the possibility of using such instruments to determine the $C_2H_6:CH_4$ in field conditions (Rella et al. 2015; Assan et al. 2017; Lopez et al. 2017, Lowry et al. 2020). In the study of Assan et al. (2017), a CRDS G2201 -i was located in a fixed location nearby to natural gas facilities. Over the course of two weeks, dried ambient air was measured simultaneously by CRDS G2201 -i and GC-FID, using the 10-minute averages for 16 “events” of high methane mixing ratios lasting more than one hour. The $C_2H_6:CH_4$ allowed to separate plumes of biogenic or thermogenic origin.

70 Rella et al. (2015) and Lopez et al. (2017) used the CRDS instrument as part of a mobile setup enhanced with a storage tube, called AirCore (Karion et al. 2010). This storage tube allows sequential reanalysis of air at an improved time resolution and hence precision. The mobile measurements can be made in two modes using this setup. During the “monitoring mode” the air is injected to the analyzer and to the open-ended AirCore at the same time. In the “replay mode”, air from the AirCore is measured. Using the AirCore with a lower flow rate increases the sampling frequency. The replay mode is only used after the

75 observation of a methane plume (Rella et al. 2015; Lopez et al. 2017; Hoheisel et al. 2019). Rella et al. (2015) observed $C_2H_6:CH_4$ ranging from 0.12 for gas sources and 0.22 for oil wells in the Uintah Basin (Utah, US). In this study, the main purpose is to evaluate the performances of the CRDS G2201 -i and the applicability of making short-term, direct, continuous and mobile measurements of ethane in methane-enriched air, with sufficient precision during near-source surveys. Our motivation is to perform both isotopic and ethane measurements with only one instrument in the field in

80 order to improve the partition of methane sources without the need for an additional analyzer. We aim to provide a protocol useful for other scientific teams, that do not possess an analyzer designed for ethane measurements, but already have the CRDS G2201 -i and intend to use it under field conditions for measuring both $\delta^{13}CH_4$ and ethane to methane ratio. To achieve this goal, the first step consists of laboratory tests to calculate the calibration factors and also to check the instrument performance under laboratory conditions, extending preliminary work by Assan et al. (2017). The second, novel step evaluates

85 the performances of the instrument during mobile field measurements in a controlled release experiment. Therefore, a mixture with known $C_2H_6:CH_4$ and CH_4 emission flux was released and compared to measured ratios from CRDS G2201 -i and LGR UMEA. In the third step, the instrument has been evaluated in real field conditions, during car-based surveys conducted at gas compressor stations and one landfill. In this step, measured values were compared to values from gas chromatography and those in natural gas provided by the operator of the gas compressor stations. These extensive tests allow a full characterization

90 of the CRDS G2201 -i instrument for car-based ethane measurements and highlighted the limitations of this instrument when measuring $C_2H_6:CH_4$. After presenting material and methods for these three steps (Sect. 2), their results are presented (Sect. 3) and discussed (Sect. 4).

2. Material and Methods

The CRDS G2201 -i (Picarro Inc., Santa Clara USA) used during this study was originally designed for measurement of the mixing ratios of $^{12}C^{16}O_2$, $^{13}C^{16}O_2$, $^{12}C^1H_4$, $^{13}C^1H_4$ and $^1H_2^{16}O$ (hereafter H_2O). It operates in three spectral lines: 6057, 6251 and 6029 cm^{-1} . As there is an interference of $^{12}C_2^1H_6$ (hereafter C_2H_6) on $^{13}CH_4$ in the absorption spectra, this instrument also

measures C₂H₆ to correct this interference. Interferences with other species is presented in Appendix A. By default, C₂H₆ is not intended for use by standard users. Thus, the measured C₂H₆ mixing ratio is not corrected nor calibrated and it is stored in private archived files. To use ethane measurements per se, measured C₂H₆ values must be first corrected for interferences with ¹²C¹⁶O₂ (hereafter CO₂), H₂O and ¹²CH₄. Different interference correction factors are needed in the absence or presence of water vapor (Assan et al. 2017). These correction factors are used and discussed in light of our new tests in Sect. 2.1.1. The water sensitivity test is also described in Sect. 2.1.1.

To ensure comparability and traceability of the ethane measurement, ethane measured by the G2201-i must eventually be linked to a widely used scale. Therefore, ethane values were calibrated before use (Sect. 2.1.2). Finally, C₂H₆ values, corrected and calibrated, can be used to determine the C₂H₆ correction on δ¹³CH₄ mixing ratio or, as in this study, to determine the ethane to methane ratio. Figure 1 shows the necessary procedure before using C₂H₆ measured by CRDS G2201-i.

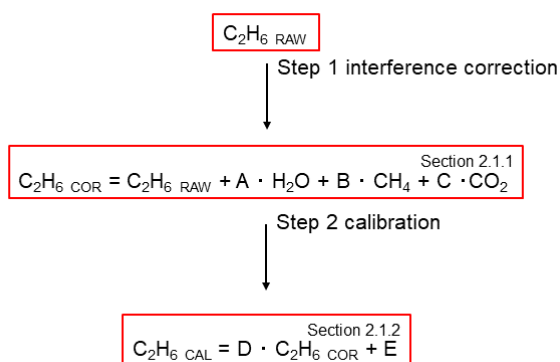


Figure 1 Flow chart of steps to use C₂H₆ measured by CRDS G2201-i. The number in the corner corresponds to the subsection where methods of each step are presented.

The same device (CRDS G2201-i CFIDS 2072) was used as by Assan et al. (2017) allowing the determination of possible long-term drift in calibration factors. Additionally, as part of the laboratory tests, continuous measurement repeatability (CMR, used as a precision in Yver Kwok et al., 2015) and Allan variance (Allan, 1966; Yver-Kwok et al., 2015) were determined for the working gases with different C₂H₆ mixing ratios (Sect. 2.1.3). Results obtained for CRDS G2201-i are compared with performances of CRDS G2132-i, which also can measure C₂H₆ as additional feature (Rella et al. 2015) and CRDS G2210-i, which is designed for C₂H₆ measurements. The characteristic of each instrument is presented in Table 1.

115

Table 1 Characteristics of the instruments used during the study

Analyzer	species	Rise/fall time	Measurements interval [s]	CH ₄ operational range [ppm]	C ₂ H ₆ operational range [ppm]
CRDS	CO ₂ , δ ¹³ CO ₂ , CH ₄ ,	~30 s	3.7	1.8 – 12	NaN
G2201-i	δ ¹³ CH ₄ , H ₂ O, C ₂ H ₆ (optional)				
CRDS	CO ₂ , CH ₄ , δ ¹³ CH ₄ , H ₂ O,	~30 s	2	1.8 – 12	NaN
G2132-i	C ₂ H ₆ (optional)				
CRDS	CO ₂ , CH ₄ , δ ¹³ CH ₄ , H ₂ O,	NaN	1	1.5 – 30	0 – 100
G2210-i	C ₂ H ₆				

2.1. Laboratory setup

2.1.1. Sensitivity of interference correction parameters to humidity

The cross sensitivities with H₂O, CO₂ and ¹²CH₄ induce a bias in raw C₂H₆ observed by CRDS G2201-i. Assan et al. (2017) provided the strategy to determine C₂H₆ correction factors to account for these interferences. During the experiment, the C₂H₆ mixing ratio of measured gas mixture was constant, while the mixing ratio of interfering species was changed and controlled using a setup similar to the one presented on Fig. 2 in the Sect. 2.1.2. During one measurement set, the concentration of only one interfering species was changed, while the concentration of other species remained constant. The measurement set was repeated while varying concentrations of H₂O, CH₄ and CO₂ were adjusted. Using linear regression, the test yielded values for the interference correction factors A, B, C in Eq. 1:

$$C_2H_6_{cor} = C_2H_6_{raw} + A \cdot H_2O + B \cdot CH_4 + C \cdot CO_2 \quad (1).$$

The interference of other species on C₂H₆ also changes in relation to the water vapor level in the measured sample. In Assan et al. (2017), the correction factors were determined for two different CRDS G2201-i devices (Assan et al. 2017, Table 2). According to that study, if the water vapor level in the measured gas is less than 0.16% (“low humidity case”), then interference correction factors are the same for both devices. In the presence of water vapor (=>0.16 %, “high humidity case”), the correction factors were different for each device. The threshold of 0.16 % corresponds to 26.14 % of relative humidity in standard conditions of temperature and pressure. Due to these differences, drying air is strongly recommended before making measurements (Assan et al., 2017). In this work, the correction factors determined by Assan et al. (2017) are used.

Table 2 Interference correction on C₂H₆ (Assan et al., 2017)

	CFIDS 2072			CFIDS 2067		
Humidity	A [ppm C ₂ H ₆ / % H ₂ O]	B [ppm C ₂ H ₆ / ppm CH ₄]	C [ppm C ₂ H ₆ / ppm CO ₂]	A [ppm C ₂ H ₆ / % H ₂ O]	B [ppm C ₂ H ₆ / ppm CH ₄]	C [ppm C ₂ H ₆ / ppm CO ₂]
Low humidity	0.44 ± 0.03	8 · 10 ⁻³ ± 2 · 10 ⁻³	1 · 10 ⁻⁴ ± 1 · 10 ⁻⁵	0.44 ± 0.03	8 · 10 ⁻³ ± 2 · 10 ⁻³	1 · 10 ⁻⁴ ± 1 · 10 ⁻⁵
High humidity	0.7 ± 0.03	0	3.8 · 10 ⁻⁴ ± 2 · 10 ⁻⁵	1 ± 0.01	0	3.9 · 10 ⁻⁴ ± 2 · 10 ⁻⁵

As a part of the laboratory test, we ran a water vapor sensitivity test to revise the parameters of the interference correction (Eq. 1, Table 2) in wet air. The target gas (hereafter referred to Target Gas 1) had a typical ambient C₂H₆ atmospheric mixing ratio. During the test, Target Gas 1 was progressively humidified (0 to 3 %) by steps of 0.25 %, using a liquid flow controller (Liquiflow, Bronkhorst, Ruurlo, the Netherlands) and a mass flow controller (MFC, Bronkhorst) coupled to a controlled evaporator mixer (CME, Bronkhorst). Each step lasted 20 minutes and the cycle was repeated three times. During data analysis, the interference correction factors from Assan et al. (2017) were applied (Table 2). Three cases were tested: no correction, high humidity case and low humidity case (except for the first step with dry air, where only the low humidity correction was applied).

2.1.2. Ethane Calibration Factors

The calibration factors are calculated as the slope (factor D) and intercept (factor E) of the linear regression of measured (subscripted “cor”) C₂H₆ versus true C₂H₆ (“cal”) in Eq. (2).

$$C_2H_6_{cal} = D \cdot C_2H_6_{cor} + E \quad (2).$$

Here, the reference gases are prepared using the approach presented by Hoheisel (2018), where a synthetic gas mixture of known C₂H₆ (“target”), is diluted with a gas (“dilution”) with known CO₂ and CH₄ mixing ratios. “True” C₂H₆ mixing ratio is obtained by applying the following equation:

$$C_2H_6_{true} = \left(1 - \frac{1}{2} \left(\frac{CH_4_{meas}}{CH_4_{dilution}} + \frac{CO_2_{meas}}{CO_2_{dilution}} \right) \right) \cdot C_2H_6_{target} \quad (3).$$

where C₂H_{6 true} is the ethane mole fraction in the reference gas obtained by mixing air from the target and dilution cylinders with concentrations of species X (respectively labelled X_{target} and X_{dilution}) using MFCs. CH_{4 dilution} and CO_{2 dilution} are the mixing

ratio of the dilution gas. $CH_{4,meas}$ and $CO_{2,meas}$ are average measured mixing ratios after dilution. This calculation is repeated for different $C_2H_6:CH_4$ ratios, determined using the MFCs.

The calibration factors are calculated with the $C_2H_6:CH_4$ gradually increased from 0.00 to 0.15 and measured in steps of 20 minutes. This measurement cycle is repeated three times. The second target gas has an ethane mixing ratio ~52 ppm (hereafter referred to as Target Gas 2) and is mixed with the dilution gas via two MFCs (Fig. 2). As the flow rate of the measured gas is greater than the instrument's inlet allowance, an open split is installed before the analyzer to vent the generated mixture and maintain an ambient pressure at the instrument inlet. The central 15 minutes of each 20-minute measurements are kept for further analysis. Then, the calibration factors are calculated as a regression slope and an intercept of the linear fitting, of theoretical (Eq. 3) against measured C_2H_6 with already applied correction factors from Eq. (1). The slope and intercept are used as factors D and E in calibration equation (Eq. 2). This test was repeated twice: in January 2018 and April 2019.

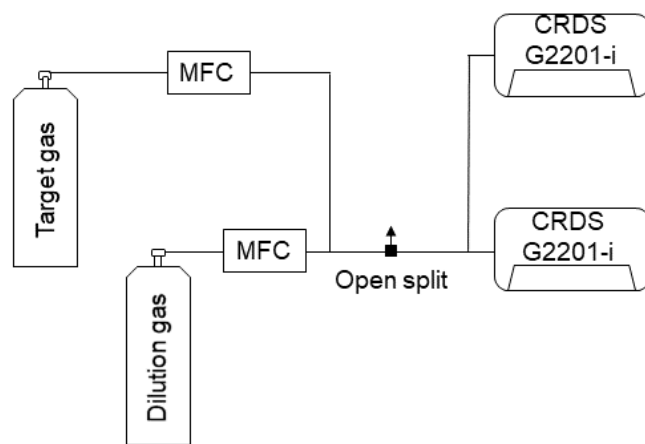


Figure 2. Experimental setup used during laboratory tests.

2.1.3. Precision and Allan Variance

CMR is calculated as the standard deviation (SD) over different averaging times (see Yver Kwok et al., 2015). The CMR test has been made by measuring a working gas continuously over 24 hours. CMR is calculated as standard deviation over different averaging times (see Yver Kwok et al., 2015). This test was applied twice: first using a working gas with ambient air amount of ethane (hereafter referred to as Target Gas 3) and second, with a gas mixture where $C_2H_6:CH_4$ ratio was equal to 0.05 (mixture of Target Gas 2 and 3). This test is to determine the CMR and instrument noise in the absence or presence of ethane. The Allan deviation was then calculated to determine the noise response of the instrument over different averaging times. Typically, the Allan deviation decreases for increasing averaging time. However, depending on the instrument, with increasing of averaging time, instrument drift can lead to the increase of the Allan deviation. Thus, the optimal averaging time can be then identified (Allan, 1966).

Further to CMR and Allan variance tests Additionally, another target gas (hereafter referred to as Target Gas 4), traceable to the WMO X2004A CH₄ scale, was sampled for 20 minutes, with a CH₄ mixing ratio about 10 000 ppb and a C₂H₆ mixing ratio about 1 000 ppb. This test allowed us to determine the linearity and short-term precision of the instrument for a gas with a higher mixing ratio than that of ambient air, both of C₂H₆ and CH₄.

2.1.4. Time drift

The drift of the C₂H₆ baseline between December 2018 and May 2019 was investigated. A known working gas (dry atmospheric mixing ratio of CH₄ and C₂H₆), hereafter referred to as Target Gas 5, was measured during 11 randomly chosen days, 20 times over the course of that period and for about 20 minutes each time. That measurement was made systematically as part of the mobile-measurement protocol (described below). The gas was measured before and after surveys to check instrument stability and the influence of power cycling.

2.2. Mobile measurement setup

This section describes the car-based instrument setup. The general principle of the setup is comparable to previous mobile methane work (e.g., Hoheisel et al., 2019; Lopez et al., 2017; Rella et al., 2015).

As the analyzer was not originally designed for mobile measurements, the vibrations induced by the car motion cause noise in the instrument readouts of C₂H₆ mixing ratio. Such a constraint can be overcome using two approaches. Firstly, by stopping the car and spending time inside the plume. Secondly, by sampling air using the AirCore (Karion et al. 2010; Rella et al. 2015; Lopez et al. 2017) while moving through the plume and eventually reinjecting the AirCore's air into the analyzer while stopped. Previously, the AirCore tool was successfully used as part of a mobile measurement setup to determine the isotopic composition of the methane source (Rella et al. 2015; Hoheisel et al. 2019; Lopez et al. 2017) and to determine the C₂H₆:CH₄ (Lopez et al. 2017).

Here, both stopping inside the plume and AirCore replay approaches were used during the mobile measurements. The AirCore used in this study is made of 50 m Dekabon storage tube. In our setup, the instrument flow rate in the monitoring mode was increased to 160 mL min⁻¹ (by default, in CRDS G2201-i the flow rate is equal to 25 mL min⁻¹) to achieve faster instrument response during mobile measurements. The replay mode was chosen as the optimal solution between increasing the number of measurement points and having enough air for each zone sampled. Here, in the replay mode, using the needle valves, the flow rate decreased about 3 times. With 50 mL min⁻¹ flow rate, one AirCore analysis lasted about ten minutes. In the replay mode, the car was stopped to avoid possible increase of instrumental noise due to car vibration. While stopping inside the plume, the data was collected in the monitoring mode with the vehicle engine stopped.

For all mobile measurements, the background mixing ratios both for CH₄ and C₂H₆ were calculated as the 1st percentile of the data sampled just before and just after the plumes. Then data with CH₄ enhancements above the background are analyzed further. The C₂H₆:CH₄ was calculated for each enhancement as the slope of the linear regression of C₂H₆ against CH₄. Fitting of the C₂H₆ versus CH₄ was calculated as a linear regression type II (allowing for uncertainty in both x- and y-axis) with the

ordinary least squares (OLS) method. Before fitting, both CH₄ and C₂H₆ were calibrated and C₂H₆ was also corrected (Fig. 1).
215 The measurements setup and data treatment protocol were the same for the controlled release experiment (Sect. 2.3) and for the field experiment (Sect. 2.4).

2.3. Controlled release experiment setup

In September 2019, over a period of five days, a gas release experiment was conducted by the National Physical Laboratory (NPL, UK) and the Royal Holloway University of London (RHUL, UK). The experiment took place at Bedford Aerodrome,
220 UK. A description of the experimental setup configuration can be found in Gardiner et al. (2017). The goal was to evaluate the methods for calculating C₂H₆:CH₄ ratios, gas flow rate and isotopic composition during local mobile measurements. Each release lasted about 45 minutes. During the experiment, the parameters of each release: C₂H₆:CH₄ (0.00 to 0.07), emission flux (up to 70 L min⁻¹) and the source height (ground level or ~4 m elevation) were varied. Here, results from 10 releases with known parameters and varying C₂H₆:CH₄ are presented.

225 Seven releases were measured using the mobile setup (AirCore and standing in the plume). Air was dried before entering the analyzer using a magnesium perchlorate cartridge. Due to the limited time of the releases, the time spent within the plume was approximately 15 to 20 minutes. Raw data was corrected according to Eq. (1), using the low humidity case, and the calibration factors (Eq. 2) were applied.

Three other releases were sampled using 5-liter sample bags (Flexfoil, SKC Inc.) only. Between 1 and 3 bag samples were
230 collected inside the plume and one was collected outside the plume as a background. Afterward, bags samples were measured in the laboratory using the CRDS G2201-i. The samples were measured without drying and the correction was applied for water vapor higher than 0.16 % (“high humidity case”). Then, the C₂H₆:CH₄ enhancement ratio was calculated separately for each bag and also as a regression slope of C₂H₆ against CH₄ values. The results are presented in Appendix C.

2.4. Field setup and experiment

235 As a final step to evaluate the G2201-i performance while mobile and under field conditions, the mobile-measurement setup, described in Sect. 2.2 has been used during surveys made in the Paris area. During spring and summer 2019, 6 surveys focused on three gas compressor stations (one survey for one of them and two surveys for the other two) and one landfill (one survey). All measurements were made outside of the sites from the closest public road. To measure the car was stationary inside the plumes for about 35 minutes and the central 30 minutes of data were analyzed. Part of the measurements were made with
240 magnesium perchlorate as a dryer before the instrument inlet and part of the measurements were made without a dryer. This allow for the additional verification of the water influence on the ethane to methane ratio observed by the CRDS G2201-i. For each measurement site, three previously evacuated 800 mL flask samples were also taken to be measured within three weeks after sampling at LSCE (Assan et al., 2017). Measurements were performed with a GC-FID (HP6890) equipped with a CP-Al₂O₃ Na₂SO₄ column and coupled to a preconcentrator (Entech 2007) to allow automatic injection. A standard cylinder
245 (Messer) containing 5 non-methane hydrocarbons including ethane was used to check the stability of the instrument, while

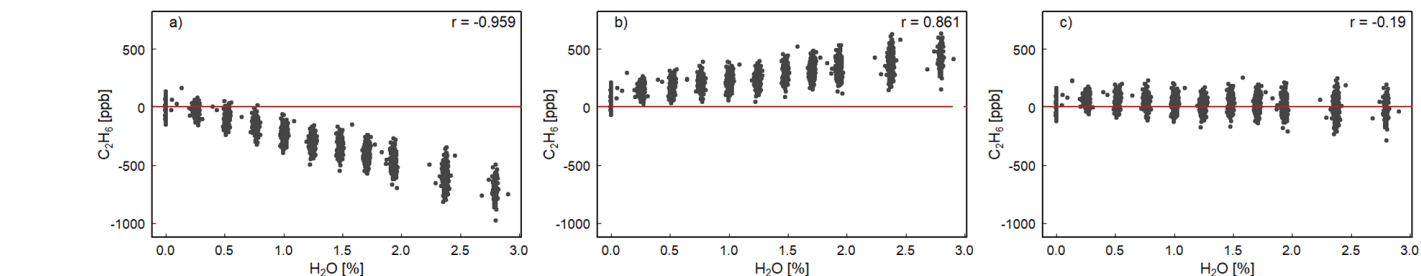
calibration was performed against a reference standard from NPL (National Physics Laboratory, UK). A previous characterization of the system had shown that the detection limit covers a few ppt, the reproducibility of measurements is about 2 % and the precision is better than 5 % (Bonsang and Kanakidou, 2001).

3. Results and discussion

250 3.1. Laboratory work

3.1.1. Sensitivity of interference correction parameters to humidity

We estimated the robustness of Eq. (1) interference correction parameters for H₂O, CO₂ and CH₄. Figure 3 shows that without interference correction, the C₂H₆ mixing ratio is underestimated and the instrument displays a negative correlation with water vapor ($r = -0.96$). In the high humidity case interference correction, C₂H₆ is overestimated and increases with increasing water vapor ($r = 0.86$). Regarding the low humidity interference correction case, C₂H₆ shows the smallest dependency on water vapor ($r = -0.19$). Applying the low humidity correction values, the C₂H₆ average value is 28 ± 61 ppb (standard error 22 ppb), which is similar to the C₂H₆ average value obtained during CMR test (33 ± 51 ppb for raw data), in dry air (Sect. 3.1.3). Overall, according to this study, after applying low humidity correction values, the water vapor has the smallest impact for observed C₂H₆ mixing ratio and its averaged value is similar to the one obtained in the absence of water vapor. Therefore, the correction factors, determined for the low humidity case, should also be used in water vapor presence. Our results differ from the findings of Assan et al. (2017), where changing values of the interference correction depending on the humidity were observed. In the absence of further tests to conclude, we recommend drying air for the C₂H₆ measurements with the CRDS G2201-i instrument. Details of the water vapor tests are presented in Appendix A.



265 **Figure 3. H₂O influence on corrected C₂H₆. Water vapor is increased in small steps for 4 hours while measuring Target Gas 1. The three panels show the result of applying different water correction protocols for next steps: a) no correction b) high humidity interference correction c) low humidity interference correction. In all cases, for H₂O= 0.00%, C₂H₆ is corrected using low humidity interference correction. The red line represents 0 ppb.**

3.1.2. Ethane Calibration Factors

270 Here, the calibration slope (factor D) and intercept (factor E) in Eq. (2) were calculated using linear fitting of true C₂H₆ versus observed C₂H₆. The calibration factors D and E were determined after applying the interference correction (Eq. 1). Table 3

compares new calibration factors for the specific CRDS G2201-i device CFIDS 2072 obtained in 2018 and 2019 with previous results by Assan et al. (2017). The calibration factors D and E have not changed significantly between 2015 and 2019, indicating that the performance of the instrument remains relatively stable over time.

275 **Table 3. Summary of the calibration factors for CRDS G2201-i device CFIDS 2072**

C ₂ H ₆ calibration	Slope Factor D	Intercept [ppm] Factor E	Reference
February 2015	0.49 ± 0.03	0.00 ± 0.01	(Assan et al. 2017)
October 2015	0.51 ± 0.01	-0.06 ± 0.04	(Assan et al. 2017)
January 2018	0.51 ± 0.01	-0.03 ± 0.01	This study
April 2019	0.54 ± 0.01	-0.03 ± 0.01	This study

3.1.3. Precision and Allan Variance

We determined the instrument CMR and Allan variance by measuring Target Gas 3 for 24 hours. The same gas was also measured by GC-FID coupled to a preconcentrator, yielding a C₂H₆ mixing ratio of 2.2 ± 0.1 ppb. Using the CRDS G2201-i, the corrected and calibrated value is different and steadily equals 33.2 ± 1.7 ppb over the 24-hour duration. This value suggests a bias of 31 ppb at low C₂H₆ concentrations, which is on the level observed for the ambient air. This bias comes probably from the fact that Target Gas 2 concentration is not known with a precision good enough, leading to errors when diluting to very low concentrations. To remove this bias, C₂H₆ mixing ratio were taken as enhancements over background during mobile measurements (Sect. 3.2 and 3.3). For more demanding purposes, a calibration strategy with more measurement points in the lower C₂H₆ concentration range and calibration tanks with lower uncertainty should be used.

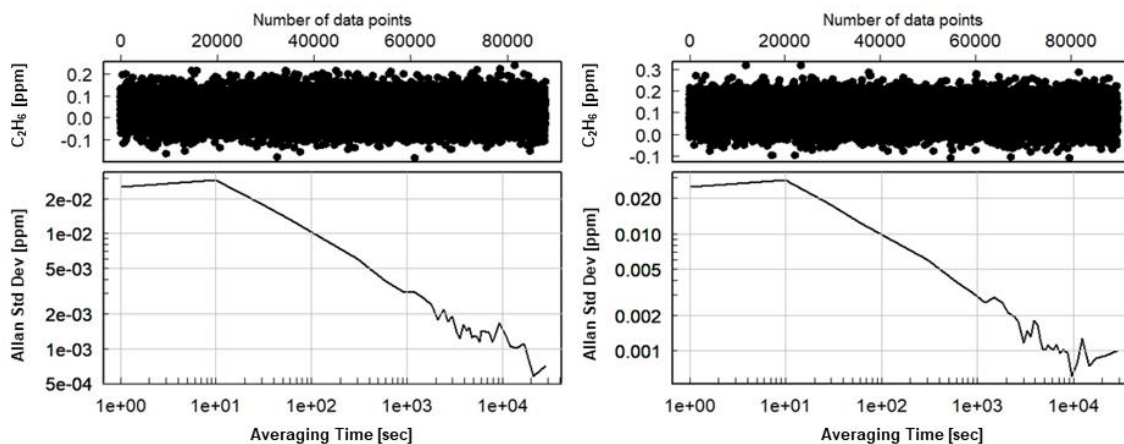
280 Following the 24 hour test, CMR and Allan deviation (Fig. 4) are calculated for target gases with different C₂H₆ mixing ratios: low mixing ratio (Target Gas 3), 100 ppb (mixture of Target Gas 2 and 3) and 1 000 ppb (Target Gas 4). In all cases, increasing the ethane mixing ratio does not affect the determined CMR and Allan deviation. Looking at the raw data (one data point every 3.7 s) for different mixing ratios, CMR and Allan deviation are ~ 50 ppb and 25 ppb, respectively. Increasing averaging time improves these parameters and for 1 minute average, both CMR and Allan deviation achieve ~ 13 ppb. For the CRDS model

285 G2132-i, also not originally designed for ethane measurements (Rella et al. 2015), the CMR in 1 minute is ~ 20 ppb and Allan deviation in 1 minute is ~ 25 ppb. Currently, new CRDS instruments designed for ethane measurements are available, for example, the CRDS 2210-i, which also measures δ¹³CH₄. Recently (in February 2020), at the ICOS Atmosphere Thematic Centre (ATC) Metrology Laboratory (MLab), the CRDS G2210-i was tested and for C₂H₆ its CMR and Allan deviation are equal to 0.9 ppb and 0.8 ppb in 1 minute (ATC Mlab, personal communication) which is much lower in comparison to our

290 analyzer. However, as stated before, our motivation is to evaluate if any G2201-i, (including former ones still operating in many places) can provide scientifically useful ethane measurements. The comparison between the instruments are presented in Table 4.

Table 4. CMR and Allan deviation for G2201-i G2132-1 and G2210-i.

Averaging time	Id	G2201-i Low C ₂ H ₆	G2201-i ~100 C ₂ H ₆	G2201-i ~1000ppb C ₂ H ₆	G2132-i (Rella et al., 2015)	G2210-i (ATC MLab) (personal communication)
Raw data	CMR [ppb]	51	50	50	NA	4.6
	Allan deviation [ppb]	25	25	26	NA	NA
10 second	CMR [ppb]	30	29	30	NA	NA
	Allan deviation [ppb]	29	29		NA	NA
1 minute	CMR [ppb]	13	12	12	20	0.9
	Allan deviation [ppb]	13	12	12	25	0.8



300 **Figure 4. Allan deviation for corrected and calibrated C₂H₆. Left: Measurement of working gas with ambient C₂H₆ mixing ratio (Target Gas 3), right: measurement of the mixture of working gas with ~100 ppb of C₂H₆ (mixture of Target Gas 2 and 3).**

With a possible 30 ppb bias and a CMR of 50 ppb, the CRDS G2201-i cannot be used to measure an absolute value of ethane in ambient air. However, this instrument can be used to observe ethane enhancement near the source and to estimate C₂H₆:CH₄ ratios. From these numbers, we can deduce that the smallest enhancement that the analyzer can measure with significant
 305 precision at the highest possible data acquisition frequency is above 50 ppb. This value was obtained both for gas with a low and high C₂H₆ mixing ratio (~100 ppb and ~1 ppm). One can assume that a C₂H₆ enhancement is significant when the maximum C₂H₆ mixing ratio at the peak is higher than 2xCMR, i.e., 100 ppb above background.

3.1.4. Time drift

Figure 5 shows the time series of Target Gas 5 measurements with an ambient amount of C_2H_6 during the period of December 2018-May 2019. The C_2H_6 mixing ratio measurements do not change significantly here. Their mean is equal to 23 ± 12 ppb (Fig. 5). It is in contrast to Assan et al. (2017), where a time drift of the baseline was observed. This difference can be caused by the fact that during previous studies, the drift was determined for corrected but uncalibrated data. Here, we applied both correction and calibration before determination of time drift. Moreover, during studies of Assan et al. (2017), bigger changes in determined calibration factors were observed over time (i. g. 60 ppb difference of factor E). Our tests showed that the ethane measurements are stable over annual timescales once proper interference correction and calibration applied. Again, measuring dry air is recommended (Sect. 3.1.1.). In the following analyses, no baseline drift correction is applied. It should be noted that the C_2H_6 concentration of Target Gas 5 was in the range of clean continental air (0.5-2 ppb). The observed mean C_2H_6 mixing ratio for Target Gas 5, equal to 23 ppb, is overestimated. This is comparable to the 31 ppb bias observed during 24 hours measurements of Target Gas 3 (Sect. 3.1.3).

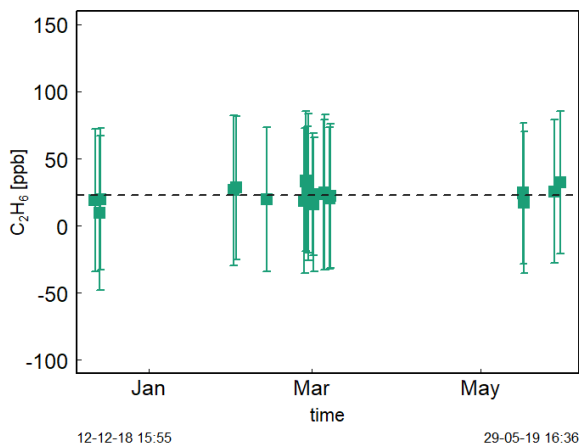
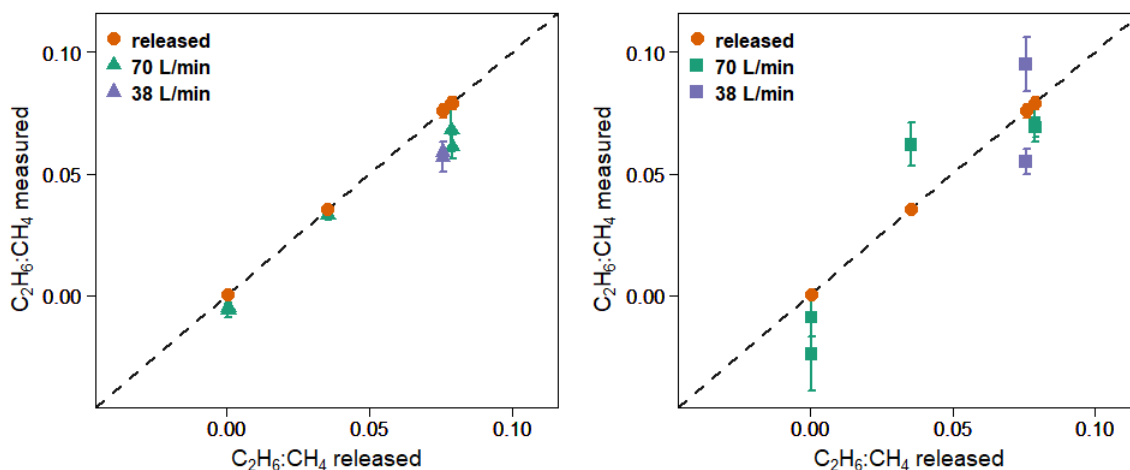


Figure 5. Target Gas 5 20-minute measurements over half a year. For each measurement point: squares represent averaged value, error bars – 1 standard deviation

3.2. Controlled release experiment

Figure 6 and Table 5 show $C_2H_6:CH_4$ ratios, expressed in $ppb\ ppb^{-1}$, measured in situ during the controlled release experiment (see Sect. 2.2). During these 7 releases, the $C_2H_6:CH_4$ was set to ~ 0.032 for one release, ~ 0.00 for two releases and ~ 0.07 for four releases. In the case, when $C_2H_6:CH_4 = 0.00$, ethane was not released while methane was released. Possibly, observed ethane mixing ratio could be due to ethane impurity in the released methane (however, no ethane was detected using the LGR instrument during the zero ethane releases). For measurements during which the car stopped inside the plume, most of the data from the CRDS G2201-i was lower than known emitted $C_2H_6:CH_4$ ratio, (mean absolute deviation = 0.011, standard deviation

330 = 0.004) with residuals in the range -0.018 to -0.002 for raw data (Table 5). The residuals were calculated as a difference between measured and released $C_2H_6:CH_4$. The observed underestimation can be caused by a systematic bias observed during laboratory test or an insufficient number of measurement points (15-20 minutes of measurement). For AirCore measurements, there are more discrepancies than for the stationary in-plume situation, with residuals in the range -0.025 to 0.027 (mean absolute deviation = 0.017, standard deviation=0.009). Thus, the stationary in-plume situation setup shows data with less
335 spread than AirCore results. These results show that in the case of $C_2H_6:CH_4$ measurements, standing inside the plume gives results which are closer to the reality than AirCore sampling. The example of observed CH_4 and C_2H_6 mixing ratios while standing inside the plume during one of the gas releases is presented in appendix B.



340 **Figure 6. $C_2H_6:CH_4$ observed using G2201-i as a part of a mobile setup. Left: measured standing inside the plumes. Right: measured using AirCore. Red points: known released $C_2H_6:CH_4$. Error bars represent 1 standard deviation. The uncertainties of released values are invisible on the graph.**

We also investigated the sensitivity of the $C_2H_6:CH_4$ to emission rates. During releases there were two different emission rates: $38 L min^{-1}$ and about $70 L min^{-1}$. For the higher emission rate, the measurements and results were combined when the emission rates were 70, 72, and $73 L min^{-1}$. The $C_2H_6:CH_4$ was better estimated by the measurements with higher emission rates (bias is divided by more than 2 when increasing flow rate from ~ 38 to $\sim 70 L min^{-1}$). This applies to both stationary measurements
345 and using the AirCore sampler. However, only 2 different emission rates were implemented and most of the releases occurred at the rate of $70 L min^{-1}$, limiting the representativity of this sensitivity.

Table 5. C₂H₆:CH₄ with residuals for non-averaged data observed using G2201-i as a part of a mobile setup, during standing inside the plume or from AirCore measurements (AC). Background subtracted both for C₂H₆ and CH₄ before determination of C₂H₆:CH₄.

Emitted C ₂ H ₆ :CH ₄	emitted emission flux [L/min]	Source height [m]	n	LSCE CRDS G2201-i				RHUL	LGR
				C ₂ H ₆ :CH ₄	Residuals	C ₂ H ₆ :CH ₄ AC	AC residuals	Residuals C ₂ H ₆ :CH ₄	UMEA
0.0355 ± 0.0011	70	4	382	0.033 ± 0.002	-0.002	0.034 ± 0.002	0.027	-0.004	
0.0788 ± 0.0025	72	4	149	0.068 ± 0.009	-0.011	0.070 ± 0.010	-0.008	-0.006	
0.0790 ± 0.0025	73	0	220	0.061 ± 0.005	-0.018	0.063 ± 0.006	-0.010	-0.001	
0.0758 ± 0.0028	38	0	142	0.059 ± 0.004	-0.017	0.058 ± 0.004	-0.020	-0.007	
0.0758 ± 0.0028	38	4	191	0.057 ± 0.006	-0.018	0.057 ± 0.006	0.019	-0.015	
0.0005 ± 0.0006*	70	0	350	-0.005 ± 0.001	-0.005	-0.005 ± 0.002	-0.025	-0.004	
0.0005 ± 0.0006*	70	4	202	-0.006 ± 0.003	-0.007	-0.005 ± 0.004	-0.010	-0.001	
Mean residuals					-0.011		-0.004	-0.0051	

350 * Small amount of ethane impurity in the methane

In Table 5 we also report residuals of C₂H₆:CH₄ independently measured by RHUL using an LGR UMEA in an additional car. The residuals in C₂H₆:CH₄ ratios of LGR UMEA are in the range [-0.015, -0.001], and the mean value is -0.0051 (mean absolute deviation = 0.0051). Therefore, the LGR UMEA is predictably more accurate than the CRDS G2201 -i standing inside
355 the plumes (CRDS residuals in range -0.018 to -0.002 with mean -0.011). Despite the observed differences, results obtained by these two methods are comparable and both instruments were capable of resolving the variation of C₂H₆:CH₄ in this release experiment.

During the controlled release experiment, we showed that the CRDS is able to separate the different emitted mixtures through their C₂H₆:CH₄. Standing in the plume resulted in a better agreement with the real ratios, with less spread of the residuals than
360 using AirCore sampling. Increasing the AirCore sampling frequency could potentially help resolve this discrepancy.

3.3. Field work

Measurements were collected in the Paris area downwind of three gas compressor stations (referred to as Ga, Gb, Gc) and one landfill (L). All measurements in this section were done stationary inside the plume.

Table 6 presents values based on raw data (i.e. at ~3.7 s acquisition frequency). We postulate that mobile applications usually
365 aim at the highest possible acquisition frequencies. However, as the 10 s averaging increases r² fitting by about a factor two, comparison of raw data and 10 s averaged data is presented in appendix D. C₂H₆ and CH₄ mixing ratios are taken as enhancements over background (Δ). Slopes are calculated using a linear regression type II (uncertainty of x- and y-axis

influence fitting) with the ordinary least squares (OLS) method. The data is not weighted. Uncertainties reported in Table 6 and Table 7 are linear fitting slope uncertainties without adding uncertainties of C₂H₆ measurements.

370 **Table 6. Ratio measured at three different gas compressor stations (Ga, Gb, Gc) and a landfill (L); ΔCH_4 and $\Delta\text{C}_2\text{H}_6$ are defined as the difference between background value (1st percentile) and the observed value inside the peak**

id	max ΔCH_4 [ppm]	max $\Delta\text{C}_2\text{H}_6$ [ppm]	C ₂ H ₆ :CH ₄ 1 s	r ² fitting	n (data point)	Data
Ga2	1.737	0.269	0.060 ± 0.005	0.195	533	16.05.2019
Ga3	5.85	0.414	0.045 ± 0.002	0.489	495	15.07.2019
Gb3	1.454	0.260	0.052 ± 0.007	0.082	613	12.07.2019
Gb4	1.677	0.236	0.046 ± 0.008	0.086	336	12.07.2019
L	1.516	0.266	0 ± 0.006	0	712	16.05.2019
Ga1*	1.486	0.309	0.070 ± 0.013	0.162	138	16.05.2019
Gb1*	7.314	0.878	0.090 ± 0.001	0.852	811	27.05.2019
Gb2*	0.513	0.323	0.085 ± 0.022	0.024	594	12.07.2019
Gc1**	0.495	0.284	0.091 ± 0.037	0.037	711	28.05.2019

Numbers after identification letters refer to different surveys. *: Ga1, Gb1 and Gb2 (wet air) and ** Gc1 (low enhancement) are rejected from further analysis (see text).

375 Campaigns Ga1, Gb1 and Gb2 (Table 6) were made without using a dryer before the instrument inlet. Due to previous results that have cast doubts about the water vapor correction, the high humidity measurements have been rejected from further analysis. Also, in the case of measuring wet air, the ethane to methane ratio was significantly higher than expected values provided by the operator. Surveys Gb2 and Gc1 exhibited the highest uncertainties in the estimated ratio and the lowest correlation between the two species. These two surveys had the lowest CH₄ enhancements above background, about 0.5 ppm.

380 Based on error propagation (Taylor, 1997) and using 2x CMR (100 ppb) as C₂H₆ detection threshold, for a typical C₂H₆:CH₄ of interest about 0.1, the minimal CH₄ enhancement above background would therefore be equal to 1 ppm. It suggests that a minimum CH₄ enhancement of 1 ppm could be required to calculate ethane to methane ratio in field conditions with this instrument. As our observations are in line with the error propagation, we use 1 ppm CH₄ enhancement above background as a detection limit to use the CRDS G2201-i to determine ethane to methane ratio in the field conditions close to the methane
385 source, and exclude Gb2 and Gc1 from subsequent analysis.

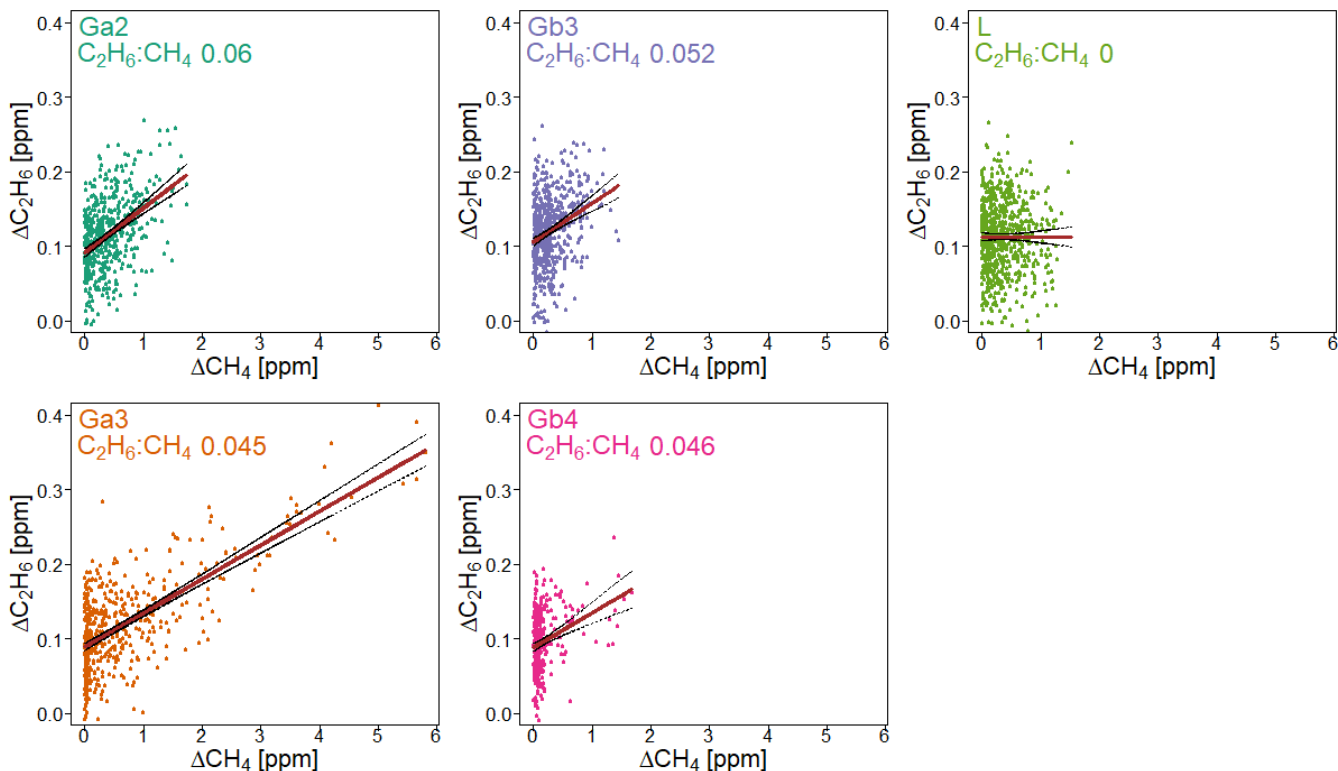


Figure 7. $C_2H_6:CH_4$ for gas compressor stations (Ga and Gb) and the landfill (L), calculated for non-averaged data. Linear fitting (red line) with confidence intervals (black lines)

Figure 7 presents observations from the valid cases. We compared the observed ratios with the values provided by the owner of the gas compressor stations. The comparison is presented in Table 7. The residuals between values measured by CRDS and values provided by the owner (considered as the “true” values) are in the range -0.006 to 0.009. This range is more symmetrically distributed around the released value than for the controlled release experiment (-0.018 to 0.002, Sect. 3.2). The uncertainty of $C_2H_6:CH_4$ measured using the CRDS G2201-i in field conditions is smaller than the differences between the ratios of CH_4 sources (e.g., biogenic sources $C_2H_6:CH_4 \sim 0.00$, natural gas leaks and compressors stations ~ 0.06 , processed natural gas liquids ~ 0.30). These results clearly show that $C_2H_6:CH_4$ measured by the CRDS G2201-i can be used to partially infer the origin of the CH_4 during mobile measurements.

Table 7. Comparison of results obtained by CRDS G2201-i with the values from the operator company.

id	CRDS 1s	Operator data	Residuals	Date
	C ₂ H ₆ :CH ₄	C ₂ H ₆ :CH ₄	C ₂ H ₆ :CH ₄	
Ga2	0.060 ± 0.005	0.051	0.009	16.05.2019
Ga3	0.045 ± 0.002	0.049	-0.004	15.07.2019
Gb3	0.052 ± 0.007	0.052	0.000	12.07.2019
Gb4	0.046 ± 0.008	0.052	-0.006	12.07.2019
L	0 ± 0.006	NA	NA	16.05.2019

400 Finally, C₂H₆ mixing ratios measured by the CRDS G2201-i are compared with results from GC-FID. Three flask samples were taken from every surveyed site and measured afterward in the laboratory using GC-FID. Then, the average of these three measures was calculated and for all sites their standard deviation is smaller than 1 ppb. On Figure 8, flask results are compared to results obtained by the CRDS G2201-i during the time of flask sampling. It should be kept in mind that due to the very short sampling time (<3s), the comparison of concentrations is only indicative. For the landfill, the C₂H₆ mixing ratio measured by
405 GC-FID is 4.9 ppb, which is higher than typical C₂H₆ mixing ratio observed for clean atmosphere (0.5-2 ppb). For Ga and Gc gas compressor stations, the C₂H₆ mixing ratio, measured by GC-FID, is 20.5 ppb and 13.7 ppb, respectively. After subtracting the determined bias, for the landfill and two compressor stations (Ga and Gc), the C₂H₆ mixing ratio measured by CRDS is still higher than the one measured by GC-FID (Fig. 8) but within the instrument noise. A different situation is observed in the case of the gas compressor station Gb where a higher C₂H₆ mixing ratio is observed. The results from flask samples are higher
410 by about 24 ppb than from CRDS analyzer after subtraction of 31 ppb bias, which is still within the instrument noise. For all sites, the CRDS measurements show a standard deviation that is almost equal to the averaged value over the sampling time. It is caused by the high instrument noise (~50 ppb CMR and 25 ppb Allan deviation for raw data) and short sampling time (less than one minute).

Field work allowed us to compare our measurements with the operator values and GC measurements. This confirms that this
415 instrument can distinguish between sources and that it agrees within its uncertainty with more precise methods such as GC.

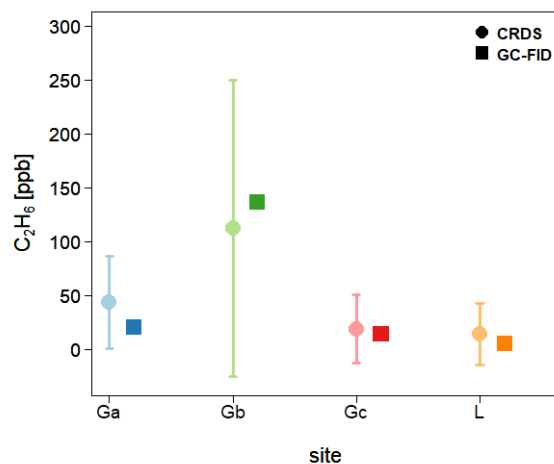


Figure 8. Comparison of the C_2H_6 mixing ratio measured in-situ by CRDS G2201-i and in the laboratory by GC-FID from flask measurements. CRDS G2201-i measurements during the time of flask sampling. Uncertainties (1 SD) are indicated both for CRDS and GC-FID.

4. Synthesis and discussion: overall comparison with other instruments and methods

420 We determined that using the CRDS G2201-i in a mobile setup to measure $C_2H_6:CH_4$ in methane plumes is possible and can provide useful scientific results under specific conditions. In laboratory conditions, during measurements of gas containing C_2H_6 , the CRDS G2201-i has a better CMR (12 ppb in 1 minute) and a smaller noise calculated from Allan deviation (~10 ppb in 1 minute) than the CRDS G2132-i, another isotopic analyzer, which are equal 20 ppb and 25 ppb, respectively, in 1 minute timeframe (Rella et al. 2015). However, both instruments have lower performance than the CRDS G2210-i, designed to

425 measure C_2H_6 . For the latter instrument, both CMR and Allan deviation are smaller than 1 ppb (ATC Mlab test, personal communication). Additionally, based on a literature comparison, for both CRDS instruments, CMR and noise are higher than those obtained from the instrument based on the TLDAS method, designed for mobile measurements of C_2H_6 (as described by Yacovitch et al. 2014). For that instrument, the CMR is as low as 19 ppt in stationary conditions, and 210 ppt in motion.

The correction of the sensitivity to other species is necessary (Eq. 1) to account for the different instrument responses to a

430 water level lower or higher than 0.16 % (low and high humidity). In this study, during laboratory work, the water vapor sensitivity was evaluated and the results showed that applying interference correction factors determined for low humidity gave better results, including wet air measurements. This is in the contrary to the results obtained by Assan et al. (2017). Rella et al. (2015) noted that the measured air should contain less than 0.1 % of water vapor. Therefore, we consider that water vapour should be removed if at all possible and we recommend drying air before C_2H_6 measurements using CRDS G2201-i.

435 Previously, the CRDS G2201-i device CFIDS 2072 has only been used in stationary field work over two weeks (Assan et al. 2017) to make continuous measurements of CH_4 , $\delta^{13}CH_4$ and C_2H_6 from gas facilities. The CRDS G2201-i and GC-FID measured air simultaneously from the shared inlet and were located 200–400 m from the gas facilities (pipelines and compressors). The GC-FID used in Assan et al. (2017) was a field instrument described in Gros et al. (2011) and Panopoulou

et al. (2018) which has an overall uncertainty estimated to be better than 15%. To obtain identical timestamps as the GC-FID, corrected and calibrated CRDS data was averaged for 10 min every 30 min. Moreover, during that study, flask samples were collected and further analyzed in the laboratory. $C_2H_6:CH_4$ from flask samples allowed to distinguish methane emissions from the two pipelines. The natural gas in pipeline 1 had an ethane to methane ratio equal to 0.074 ± 0.001 and for pipeline 2 equal to 0.046 ± 0.003 . These values are in good agreement with on-site GC-FID results which reached 0.075 and 0.048 ± 0.003 , for pipeline 1 and 2 respectively (Assan et al., 2017). Thus, the laboratory values showed good agreement between field, installed in the shelter, CRDS G2201-i and GC-FID results (Assan et al. 2017).

In our study, we went one step further and considered the constraints associated with a mobile setup within a car. As the instrument noise increases during the motion of the car, we decided to stop the car for about 35 minutes inside the plume to acquire the observations. As it is not possible to stop the car in every place where measurements are made, it is a limitation for this application of the instrument, compared to other instruments able to measure C_2H_6 while moving across the plume, such as the LGR UMEA (Lowry et al. 2020) or an instrument based on the TILDAS method (Smith et al., 2015; Yacovitch et al., 2014, 2020). However, we showed that it is possible to receive reliable values during a short time (e.g. 35 minutes) and the instrument can be successfully installed inside a vehicle. Notably, having the instrument setup inside the car facilitates the measurement setup as an additional place to install the stationary instrument is not required anymore.

During our tracer release experiment, $C_2H_6:CH_4$ was calculated from measurements performed when the car was standing inside the plume. With this approach, measured ratios were underestimated. However, using the LGR UMEA instrument, designed for mobile $C_2H_6:CH_4$ measurements, some discrepancies between the measured and the released value was also observed, albeit smaller. Indeed, in the case of the LGR UMEA measurements, the residuals between measurements and released value were in the range -0.015 to -0.001, while the residuals of the CRDS G2201-i are in the range -0.018 to -0.002. It is also worth noting that Yacovitch et al. (2014), using a more precise instrument, as well reported a systematic underestimation of the C_2H_6 mixing ratio by $\sim 6\%$.

In our study, during the tracer release experiment, we compared the results obtained by stationary standing inside the plume to sampling air with an AirCore system. The absolute deviation is equal to 0.011 and 0.017 for stationary mode and AirCore mode, respectively. The residuals between released and measured values range from -0.018 to -0.002 for stationary mode and from -0.025 to 0.027 for AirCore mode. Thus, the agreement with released $C_2H_6:CH_4$ is better for measurements performed by standing inside the plumes than those obtained with the AirCore sampler. During previous studies where CRDS instruments were used (Rella et al. 2015; Lopez et al. 2017), $C_2H_6:CH_4$ was also measured using AirCore sampler. In the study made by Lopez et al. (2017) for pipelines measurements, gas flasks were also collected and measured at INSTAAR (Boulder, CO, USA) using gas chromatography. Based on CRDS measurements with the AirCore sampler, ethane to methane ratio equalled to 0.05 ± 0.01 , while the values achieved from gas chromatography reached 0.04 ± 0.001 . Overall, the AirCore sampler results were in good agreement with the results from flasks measurements.

During study made by Lopez et al. (2017), the CRDS was flushed continuously with a flowrate of 1000 mL min^{-1} controlled by a mass flow controller. During AirCore analysis, the airflow rate was equal to 40 mL min^{-1} . This change allowed increasing

the number of measurement points by 25 during the replay mode. In our study, in the monitoring mode, we flushed the CRDS instrument with a flow rate of 160 mL min^{-1} and in the replay mode, we increased the number of points only by a factor of 3. 475 These differences could contribute to explain the discrepancies between measured and released $\text{C}_2\text{H}_6:\text{CH}_4$ ratios. Further decreasing the flow rate would increase the number of sampling points and could improve the agreement between AirCore-based estimations and actual ratios, especially for small CH_4 plumes (e.g. 1-2 ppm above CH_4 background). This should be tested to determine the optimal AirCore setup for $\text{C}_2\text{H}_6:\text{CH}_4$ to improve the characterization of methane sources.

Finally, the $\text{C}_2\text{H}_6:\text{CH}_4$ ratios obtained by standing inside the plumes are accurate and allow us to separate the different releases 480 at the resolution of the conducted experiment. The results are comparable with results obtained using LGR UMEA, with agreement between measurements and reality also been confirmed during field conditions mobile measurements on gas compressor stations. During these measurements, residuals for dry air sampling were between -0.006 and 0.009. Additionally, during field work, flask samples have been taken and measured by GC-FID in the laboratory. During the time of flask sampling at the two gas compressors stations, the C_2H_6 mixing ratios were below the value of the instrument CMR (~ 50 ppb). For the 485 third gas compressor station, the C_2H_6 mixing ratio was above the detection threshold and the C_2H_6 mixing ratio measured by GC-FID was higher than measured by CRDS. Nevertheless, due to the short sampling time of the flasks, these first comparisons between flask samples measured by GC-FID and short-term CRDS field measurements are only approximate and more comparison campaigns should help to understand the discrepancies between these instruments. In all cases, the standard deviation of C_2H_6 measured by CRDS was close to the averaged value. It shows the CRDS G2201-i should not be used for 490 measurements of the absolute value of C_2H_6 mixing ratios.

Overall, using $\text{C}_2\text{H}_6:\text{CH}_4$ measured by the CRDS G2201-i, it is possible to separate methane sources between a biogenic origin ($\text{C}_2\text{H}_6:\text{CH}_4 \sim 0.00$), natural gas leaks and compressors ($\text{C}_2\text{H}_6:\text{CH}_4 \sim 0.06$, can vary between 0.02-0.17) and processed natural gas liquids ($\text{C}_2\text{H}_6:\text{CH}_4 \sim 0.3$). $\text{C}_2\text{H}_6:\text{CH}_4$ of natural gas can vary due to its origin and processing. Also, this instrument can be used to observe the possible temporal variation of $\text{C}_2\text{H}_6:\text{CH}_4$ of methane emitted from fossil fuel sources. These studies can be 495 made in the vicinity of strong emitting sources, where CH_4 plume reaches at least 1 ppm above background. Determining the exact source of methane inside the industrial site, with a lot of potential methane emitters, is more challenging to achieve. However, with regards to the results of our study, it is possible to determine the sources of the observed CH_4 plume using $\text{C}_2\text{H}_6:\text{CH}_4$ measured with a CRDS G2201-i if the differences between $\text{C}_2\text{H}_6:\text{CH}_4$ ratios are higher than 0.01.

5. Conclusions and recommendations

500 The CRDS G2201-i instrument measures $^{12}\text{CO}_2$, $^{13}\text{CO}_2$, $^{12}\text{CH}_4$, $^{13}\text{CH}_4$, H_2O and C_2H_6 , the latter being initially present to correct $^{13}\text{CH}_4$ measurements. This study investigates the possibility to perform ethane measurements with a CRDS G2201-i instrument useful for methane source apportionment. The interest is to achieve better constrain methane sources in the laboratory and in the field with two proxies but only one instrument. Before any analysis, C_2H_6 raw data must be corrected and calibrated (Fig. 1). The linearity test showed good stability over time, with only a small change of the calibration factors over 4 years. Contrary

505 to the previous studies (Rella et al. 2015; Assan et al. 2017), we do not observe any time drift of the C₂H₆ baseline. Nevertheless, regular calibrations and target measurements are recommended.

The controlled release experiment revealed a small systematic underestimation (of measured C₂H₆:CH₄ inside the plumes compared to released ones. The larger discrepancy from released C₂H₆:CH₄ occurs in the case of AirCore samplings. Due to that, we recommend standing inside the plumes instead of taking AirCore samples to measure C₂H₆:CH₄ ratios. However, 510 decreasing the flushing flow rate of the CRDS can improve the performance of the instrument during AirCore sampling and should be further investigated in future campaigns.

In this study, we find some limitations of using CRDS G2201-i to measure C₂H₆:CH₄. First of all, we found that we need at least a peak maximum of 100 ppb ethane to gain useful results to help apportioning methane sources. Additionally, the required maximum CH₄ enhancement above background should be higher than 1 ppm. This threshold is determined using error 515 propagation for a typical C₂H₆:CH₄ equal to 0.1. Under field conditions, this threshold was successfully used for C₂H₆:CH₄ close to 0.05. For weak sources with enhancements below 1 ppm, this limitation prevents providing C₂H₆:CH₄ measurements using our approach. Secondly, we have observed significant changes in observed C₂H₆ mixing ratios in the presence of water vapor and we strongly recommend drying air before making measurements.

Thirdly, due to an increase of the instrument noise during the motion of the car, it is not possible to measure C₂H₆:CH₄ when 520 moving across plumes as currently made to estimate methane emissions (e.g., Ars et al. 2017). Other “designed for mobile operation” instruments will have to be used in this case for ethane (Yacovitch et al. 2014; Lowry et al. 2020). To work around this problem, C₂H₆:CH₄ can be measured by standing inside the plumes or offline using AirCore sampling after determining the optimal flushing flow (see Sect. 2.2 and 3.2).

Despite these limitations, this study shows the possibility of using the CRDS G2201-i to measure C₂H₆:CH₄ under field 525 conditions with strong methane enhancements, using mobile platforms and receive rapid and qualitative results. Even though the instrument is not designed for C₂H₆:CH₄ measurements, after applying correction and calibration factors, when the air is dried and the methane peak maximum value is at least 1 ppm above background, the CRDS G2201-i gives results that are comparable with released values in controlled experiments and values provided by the gas compressor manufacturing company. Therefore, under these conditions, the CRDS G2201-i instrument can contribute to better constrain methane sources 530 deploying only one instrument which is possibly already available in the laboratory.

Appendix A

Rella et al (2015) quantified the influence of other organic compounds for δ¹³CH₄ using CRDS G2132, which operates in the same wavelengths as CRDS G2201-i. They also noted that ammonia was having a strong influence on ethane. No other compounds from Table 1 (e.g. CO, CH₃SH) tested in their paper were noted as having an influence. As CRDS G2132 and 535 CRDS G2201-i operate in the same wavelength, the observed interferences are similar for both instruments.

CRDS G2201-i has the possibility to measure H₂S, NH₃ and C₂H₄. Similarly, to C₂H₆ measurements, they are measured to account for their interference for δ¹³CH₄ and, similarly to C₂H₆ measurements, they should be calibrated and corrected before any use and large instrument noise is observed during their measurements. During our study, no signal above instrument noise was observed for H₂S, NH₃ and C₂H₄ so we neglected their interference. Unfortunately, with CRDS G2201-i, it is not possible to measure C₃H₈, so we cannot conclude about possible propane interference from our measures. However, as said before, no interference on ethane was noted for propane in Rella et al (2015). Thus, we assume that propane interference is negligible.

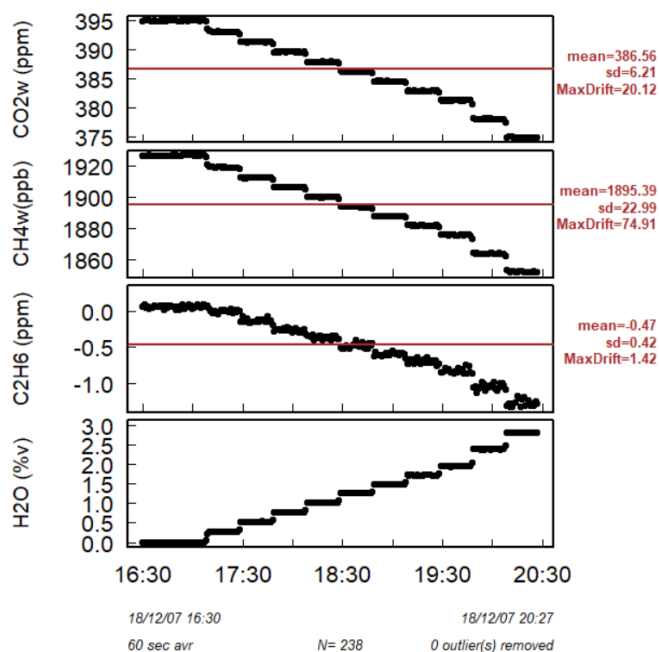
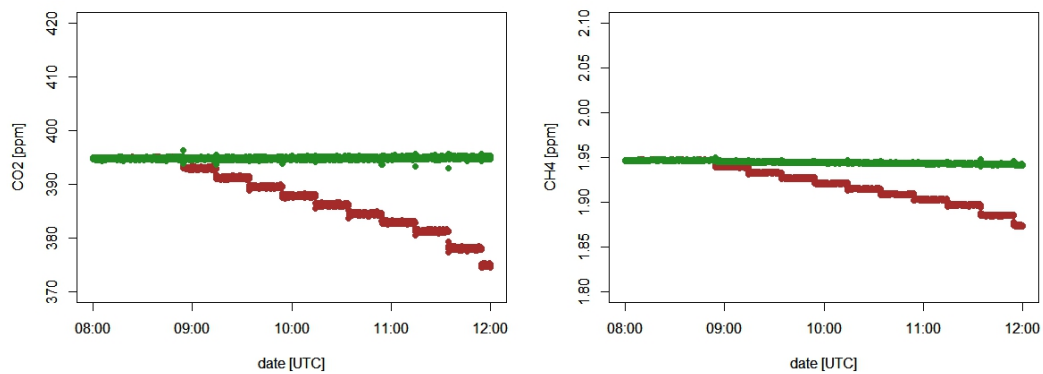


Figure A1. H₂O influence on CO₂, CH₄ and C₂H₆.

The results, presented in Fig. 3 in the article, were obtained using wet CH₄ and CO₂ values. In the next step, the analysis of the water vapor sensitivity test was repeated using dry CH₄ and CO₂ values. These dry values are corrected by default already in the instrument. For all three cases, using dry or wet CH₄ and CO₂ values did not change the C₂H₆ values, which suggests a bigger influence of H₂O than CH₄ and CO₂ on C₂H₆. When the interference correction for low humidity was applied for all steps, the average C₂H₆ mixing ratio is equal 28 ± 62 ppb and 28 ± 61 ppb for wet and dry CH₄ and CO₂, respectively. Figure A2 presents a comparison of wet and dry CO₂ and CH₄ values.



550 **Figure A2.** Dry (manufactured correction) and wet values of CO₂ and CH₄. Green – dry values, red – wet values. Left: CO₂ mixing ratio, right CH₄ mixing ratio.

Appendix B

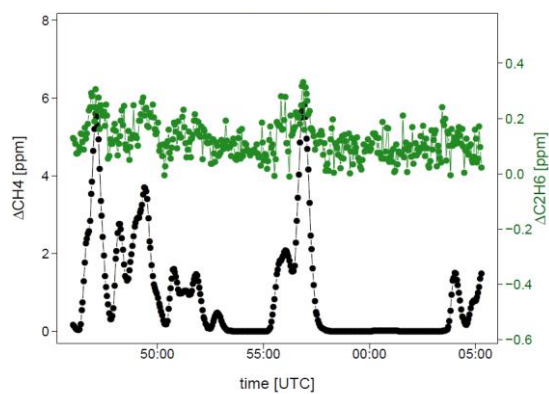
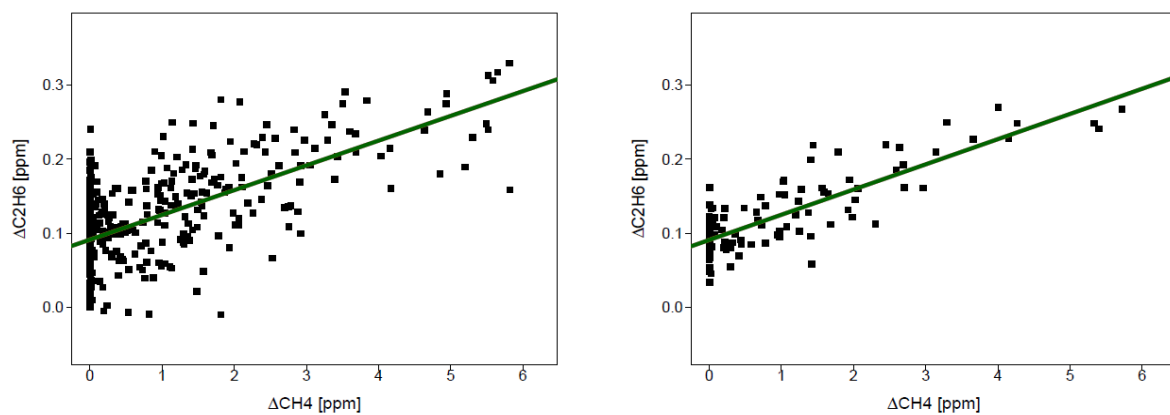


Figure B1. CH₄ and C₂H₆ mixing ratio observed during standing inside the plume



555 **Figure B2.** C₂H₆ mixing ratio vs. CH₄ mixing ratio observed while standing inside the plume. Left: non-averaged data. Right: 10 s averaged data. Green line : linear fitting

Appendix C

560 During the controlled release experiment (Sect. 2.2 and 3.2), three releases were measured offsite using 5 liter bag samples (Flexfoil, SKC Inc. flexfoil sample bags) filled with air from the plumes. The bag samples were measured afterward in the laboratory without drying. During release one and two, emitted C₂H₆:CH₄ was equal to 0.00, the third release having a C₂H₆:CH₄ about 0.032. In all cases, for background samples, the C₂H₆ mixing ratio was found higher than for the bag samples collected inside the plumes. Due to that, results from the bag samples are rejected from further analysis. There are two possible reasons for the incorrect values obtained with bag samples. First, these bags could not be adapted for storing ethane. Secondly, as the samples were wet, the H₂O, CO₂ and other species interferences on C₂H₆ could be higher and not linear. Thus, the applied interference correction did not improve the measured C₂H₆ mixing ratio.

565

Table C1 C₂H₆:CH₄ with interference correction for high humidity. * background samples

name.id	CO ₂ [ppm]	CH ₄ [ppm]	δ ¹³ CH ₄ [‰]	H ₂ O [%]	C ₂ H ₆ [ppm]	C ₂ H ₆ :CH ₄ [ppm/ppm]
1.1b	402	2.23	-47	1.25	0.27 ± 0.06	0.12 ± 0.03
1.2b	397	2.01	-47	1.22	0.27 ± 0.06	0.13 ± 0.03
1.3b	399	3.34	-45	1.22	0.39 ± 0.06	0.12 ± 0.02
1.4b*	395	1.96	-48	1.23	0.44 ± 0.06	0.22 ± 0.03
1.5b	399	2.31	-46	1.29	0.43 ± 0.06	0.19 ± 0.03
1.6b	399	5.25	-43	1.29	0.45 ± 0.07	0.09 ± 0.01
1.7b	402	5.19	-44	1.29	0.62 ± 0.09	0.12 ± 0.02
1.8b*	396	1.98	-48	1.25	0.55 ± 0.08	0.28 ± 0.04
2.1b	420	3.25	-45	1.27	0.55 ± 0.07	0.17 ± 0.02
2.2b*	397	1.97	-49	1.17	0.72 ± 0.15	0.36 ± 0.08

Appendix D

570 Comparison of raw data and 10 s averaged data from measurements in the Ile-de-France region

Table D1. Field work analysis Ga, Gb and Gc- gas compressor, L – landfill;

id	max ΔCH_4	max $\Delta\text{C}_2\text{H}_6$	1 s	r^2	10 s	r_2	n	data
Ga1*	1.486	0.309	0.070 ± 0.013	0.162	0.066 ± 0.018	0.235	138	16.05.2019
Ga2	1.737	0.269	0.060 ± 0.005	0.195	0.059 ± 0.007	0.303	533	16.05.2019
Ga3	5.85	0.414	0.045 ± 0.002	0.489	0.044 ± 0.003	0.645	495	15.07.2019
Gb1*	7.314	0.878	0.090 ± 0.001	0.852	0.091 ± 0.002	0.927	811	27.05.2019
Gb2*	0.513	0.323	0.085 ± 0.022	0.024	0.083 ± 0.029	0.044	594	12.07.2019
Gb3	1.454	0.26	0.052 ± 0.007	0.082	0.05 ± 0.009	0.15	613	12.07.2019
Gb4	1.677	0.236	0.046 ± 0.008	0.086	0.05 ± 0.011	0.174	336	12.07.2019
Gc1**	0.495	0.284	0.091 ± 0.037	0.037	0.09 ± 0.021	0.082	711	28.05.2019
L	1.516	0.266	0 ± 0.006	0	0 ± 0.007	0	712	16.05.2019

*: A1, B1 and B2 rejected from further analysis (wet air) and ** C1 rejected from further analysis (low enhancement), raw and 10 s averaged data

Data availability

575 Data from the field work and most of the laboratory tests are available on the Carbon Portal and waiting to obtain a DOI number. Data from time drift test are available on demand.

Author contribution

580 Conceptualization, S.D., J.D.P.; Methodology, S.D., J.D.P. C.Y.K., D.L., J.F., J.H., N.Y., V.G.; Software, S.D., C.Y.K., D.L.; Formal Analysis, S.D., D.L., N.Y.; Investigation, S.D., J.D.P. C.Y.K., D.L.; Resources, J.D.P. C.Y.K., P.B., J.H.; Data Curation S.D., D.L.; Writing – Original, S.D.; Draft Writing – Review & Editing, S.D., J.D.P. C.Y.K., D.L., J.F., J.H., N.Y., V.G., P.B.; Visualization, S.D., D.L.; Supervision, J.D.P. C.Y.K., P.B.

Competing interests

The authors declare that they have no conflict of interest.

Acknowledgments

585 We acknowledge our laboratory colleagues C. Philippon and L. Lienhardt, for sharing results of tests made in ATC Mlab. We thank also gratefully D. Baisnee for the measurements of flask samples on the GC-FID. We gratefully acknowledge GRTgaz company for sharing data with us and helping to improve the manuscript, especially: P. Guillo-Lohan, P. Alas, F. Bainier and J.L. Fabre.

References

- 590 Allan, D. W.: Statistics of atomic frequency standards, *Proc. IEEE*, 54, 221–230, <https://doi.org/10.1109/PROC.1966.4634>, 1966.
- Assan, S., Baudic, A., Guemri, A., Ciais, P., Gros, V., and Vogel, F. R.: Characterization of interferences to in situ observations of $\delta^{13}\text{C}\text{H}_4$ and C_2H_6 when using a cavity ring-down spectrometer at industrial sites, 10, 2077–2091, <https://doi.org/10.5194/amt-10-2077-2017>, 2017.
- 595 Aydin, M., Verhulst, K. R., Saltzman, E. S., Battle, M. O., Montzka, S. A., Blake, D. R., Tang, Q., and Prather, M. J.: Recent decreases in fossil-fuel emissions of ethane and methane derived from firn air, *Nature*, 476, 198–201, <https://doi.org/10.1038/nature10352>, 2011.
- Bonsang, B. and Kanakidou, M.: Non-methane hydrocarbon variability during the FIELDVOC'94 campaign in Portugal, *Chemosphere - Global Change Science*, 3, 259–273, [https://doi.org/10.1016/S1465-9972\(01\)00009-5](https://doi.org/10.1016/S1465-9972(01)00009-5), 2001.
- 600 Bourtsoukidis, E., Ernle, L., Crowley, J. N., Lelieveld, J., Paris, J.-D., Pozzer, A., Walter, D., and Williams, J.: Non Methane Hydrocarbon (C2-C8) sources and sinks around the Arabian Peninsula, 1–45, <https://doi.org/10.5194/acp-2019-92>, 2019.
- Dlugokencky, E.J.: NOAA/ESRL, (www.esrl.noaa.gov/gmd/ccgg/trends_ch4/) (Accessed: 14 April 2021).
- Gardiner, T., Helmore, J., Innocenti, F., and Robinson, R.: Field Validation of Remote Sensing Methane Emission Measurements, *Remote Sensing*, 9, 956, <https://doi.org/10.3390/rs9090956>, 2017.
- 605 Gros, V., Gaimoz, C., Herrmann, F., Custer, T., Williams, J., Bonsang, B., Sauvage, S., Locoge, N., d'Argouges, O., Sarda-Estève, R., and Sciare, J.: Volatile organic compounds sources in Paris in spring 2007. Part I: qualitative analysis, *Environ. Chem.*, 8, 74-90, <https://doi.org/10.1071/EN10068>, 2011.
- Hausmann, P., Sussmann, R., and Smale, D.: Contribution of oil and natural gas production to renewed increase in atmospheric methane (2007–2014): top-down estimate from ethane and methane column observations, *Atmos. Chem. Phys.*, 16, 3227–
- 610 3244, <https://doi.org/10.5194/acp-16-3227-2016>, 2016.
- Helmig, D., Rossabi, S., Hueber, J., Tans, P., Montzka, S. A., Masarie, K., Thoning, K., Plass-Duelmer, C., Claude, A., Carpenter, L. J., Lewis, A. C., Punjabi, S., Reimann, S., Vollmer, M. K., Steinbrecher, R., Hannigan, J. W., Emmons, L. K., Mahieu, E., Franco, B., Smale, D., and Pozzer, A.: Reversal of global atmospheric ethane and propane trends largely due to US oil and natural gas production, *Nature Geosci*, 9, 490–495, <https://doi.org/10.1038/ngeo2721>, 2016.

- 615 Hoheisel, A.: Characterisation of $\delta^{13}\text{C}$ source signatures from methane sources in Germany using mobile measurements, M.S. thesis, Institute of Environmental Physics, University of Heidelberg, Germany, 118 pp., 2018.
- Hoheisel, A., Yeman, C., Dinger, F., Eckhardt, H., and Schmidt, M.: An improved method for mobile characterisation of $\delta^{13}\text{C}$ source signatures and its application in Germany, 12, 1123–1139, <https://doi.org/10.5194/amt-12-1123-2019>, 2019.
- IPCC: Climate Change 2013: The Physical Science Basis. Contribution of Working Group I to the Fifth Assessment Report
620 of the Intergovernmental Panel on Climate Change, Cambridge University Press, Cambridge, United Kingdom and New York, NY, USA, 2018.
- Kort, E. A., Smith, M. L., Murray, L. T., Gvakharia, A., Brandt, A. R., Peischl, J., Ryerson, T. B., Sweeney, C., and Travis, K.: Fugitive emissions from the Bakken shale illustrate role of shale production in global ethane shift: Ethane Emissions From the Bakken Shale, *Geophys. Res. Lett.*, 43, 4617–4623, <https://doi.org/10.1002/2016GL068703>, 2016.
- 625 Lan, X., Tans, P., Sweeney, C., Andrews, A., Dlugokencky, E., Schwietzke, S., Kofler, J., McKain, K., Thoning, K., Crotwell, M., Montzka, S., Miller, B. R., and Biraud, S. C.: Long-Term Measurements Show Little Evidence for Large Increases in Total U.S. Methane Emissions Over the Past Decade, *Geophys. Res. Lett.*, 46, 4991–4999, <https://doi.org/10.1029/2018GL081731>, 2019.
- Lopez, M., Sherwood, O. A., Dlugokencky, E. J., Kessler, R., Giroux, L., and Worthy, D. E. J.: Isotopic signatures of
630 anthropogenic CH_4 sources in Alberta, Canada, 164, 280–288, <https://doi.org/10.1016/j.atmosenv.2017.06.021>, 2017.
- Lowry, D., Fisher, R. E., France, J. L., Coleman, M., Lanoisellé, M., Zazzeri, G., Nisbet, E. G., Shaw, J. T., Allen, G., Pitt, J., and Ward, R. S.: Environmental baseline monitoring for shale gas development in the UK: Identification and geochemical characterisation of local source emissions of methane to atmosphere, *Science of The Total Environment*, 708, 134600, <https://doi.org/10.1016/j.scitotenv.2019.134600>, 2020.
- 635 McKain, K., Down, A., Raciti, S. M., Budney, J., Hutyra, L. R., Floerchinger, C., Herndon, S. C., Nehrkorn, T., Zahniser, M. S., Jackson, R. B., Phillips, N., and Wofsy, S. C.: Methane emissions from natural gas infrastructure and use in the urban region of Boston, Massachusetts, 112, 1941–1946, <https://doi.org/10.1073/pnas.1416261112>, 2015.
- Panopoulou, A., Liakakou, E., Gros, V., Sauvage, S., Locoge, N., Bonsang, B., Psiloglou, B. E., Gerasopoulos, E., and Mihalopoulos, N.: Non-methane hydrocarbon variability in Athens during wintertime: the role of traffic and heating, *Atmos.*
640 *Chem. Phys.*, 18, 16139–16154, <https://doi.org/10.5194/acp-18-16139-2018>, 2018.
- Paris, J.-D., Riandet, A., Bourtsoukidis, E., Delmotte, M., Berchet, A., Williams, J., Ernle, L., Tadic, I., Harder, H., and Lelieveld, J.: Shipborne measurements of methane and carbon dioxide in the Middle East and Mediterranean areas and contribution from oil and gas emissions, <https://doi.org/10.5194/acp-2021-114>, 2021.
- Rella, C. W., Hoffnagle, J., He, Y., and Tajima, S.: Local- and regional-scale measurements of CH_4 , $\delta^{13}\text{C}$, and C_2H_6 in the
645 Uintah Basin using a mobile stable isotope analyzer, 8, 4539–4559, <https://doi.org/10.5194/amt-8-4539-2015>, 2015.
- Saunois, M., Bousquet, P., Poulter, B., Peregon, A., Ciais, P., Canadell, J. G., Dlugokencky, E. J., Etiope, G., Bastviken, D., Houweling, S., Janssens-Maenhout, G., Tubiello, F. N., Castaldi, S., Jackson, R. B., Alexe, M., Arora, V. K., Beerling, D. J., Bergamaschi, P., Blake, D. R., Brailsford, G., Brovkin, V., Bruhwiler, L., Crevoisier, C., Crill, P., Covey, K., Curry, C.,

- Frankenberg, C., Gedney, N., Höglund-Isaksson, L., Ishizawa, M., Ito, A., Joos, F., Kim, H.-S., Kleinen, T., Krummel, P.,
650 Lamarque, J.-F., Langenfelds, R., Locatelli, R., Machida, T., Maksyutov, S., McDonald, K. C., Marshall, J., Melton, J. R.,
Morino, I., Naik, V., O'Doherty, S., Parmentier, F.-J. W., Patra, P. K., Peng, C., Peng, S., Peters, G. P., Pison, I., Prigent, C.,
Prinn, R., Ramonet, M., Riley, W. J., Saito, M., Santini, M., Schroeder, R., Simpson, I. J., Spahni, R., Steele, P., Takizawa,
A., Thornton, B. F., Tian, H., Tohjima, Y., Viovy, N., Voulgarakis, A., van Weele, M., van der Werf, G. R., Weiss, R.,
Wiedinmyer, C., Wilton, D. J., Wiltshire, A., Worthy, D., Wunch, D., Xu, X., Yoshida, Y., Zhang, B., Zhang, Z., and Zhu, Q.:
655 The global methane budget 2000–2012, 8, 697–751, <https://doi.org/10.5194/essd-8-697-2016>, 2016.
- Saunois, M., Stavert, A. R., Poulter, B., Bousquet, P., Canadell, J. G., Jackson, R. B., Raymond, P. A., Dlugokencky, E. J.,
Houweling, S., Patra, P. K., Ciais, P., Arora, V. K., Bastviken, D., Bergamaschi, P., Blake, D. R., Brailsford, G., Bruhwiler,
L., Carlson, K. M., Carrol, M., Castaldi, S., Chandra, N., Crevoisier, C., Crill, P. M., Covey, K., Curry, C. L., Etiope, G.,
Frankenberg, C., Gedney, N., Hegglin, M. I., Höglund-Isaksson, L., Hugelius, G., Ishizawa, M., Ito, A., Janssens-Maenhout,
660 G., Jensen, K. M., Joos, F., Kleinen, T., Krummel, P. B., Langenfelds, R. L., Laruelle, G. G., Liu, L., Machida, T., Maksyutov,
S., McDonald, K. C., McNorton, J., Miller, P. A., Melton, J. R., Morino, I., Müller, J., Murgia-Flores, F., Naik, V., Niwa, Y.,
Noce, S., O'Doherty, S., Parker, R. J., Peng, C., Peng, S., Peters, G. P., Prigent, C., Prinn, R., Ramonet, M., Regnier, P., Riley,
W. J., Rosentreter, J. A., Segers, A., Simpson, I. J., Shi, H., Smith, S. J., Steele, L. P., Thornton, B. F., Tian, H., Tohjima, Y.,
Tubiello, F. N., Tsuruta, A., Viovy, N., Voulgarakis, A., Weber, T. S., van Weele, M., van der Werf, G. R., Weiss, R. F.,
665 Worthy, D., Wunch, D., Yin, Y., Yoshida, Y., Zhang, W., Zhang, Z., Zhao, Y., Zheng, B., Zhu, Q., Zhu, Q., and Zhuang, Q.:
The Global Methane Budget 2000–2017, *Atmosphere – Atmospheric Chemistry and Physics*, <https://doi.org/10.5194/essd-2019-128>, 2020.
- Schwietzke, S., Griffin, W. M., Matthews, H. S., and Bruhwiler, L. M. P.: Natural Gas Fugitive Emissions Rates Constrained
by Global Atmospheric Methane and Ethane, *Environ. Sci. Technol.*, 48, 7714–7722, <https://doi.org/10.1021/es501204c>, 2014.
- 670 Sherwood, O. A., Schwietzke, S., Arling, V. A., and Etiope, G.: Global Inventory of Gas Geochemistry Data from Fossil Fuel,
Microbial and Burning Sources, version 2017, *Earth Syst. Sci. Data*, 9, 639–656, <https://doi.org/10.5194/essd-9-639-2017>,
2017.
- Simpson, I. J., Sulbaek Andersen, M. P., Meinardi, S., Bruhwiler, L., Blake, N. J., Helmig, D., Rowland, F. S., and Blake, D.
R.: Long-term decline of global atmospheric ethane concentrations and implications for methane, *Nature*, 488, 490–494,
675 <https://doi.org/10.1038/nature11342>, 2012.
- Smith, M. L., Kort, E. A., Karion, A., Sweeney, C., Herndon, S. C., and Yacovitch, T. I.: Airborne Ethane Observations in the
Barnett Shale: Quantification of Ethane Flux and Attribution of Methane Emissions, *Environ. Sci. Technol.*, 49, 8158–8166,
<https://doi.org/10.1021/acs.est.5b00219>, 2015.
- Taylor, J. R.: An introduction to error analysis. The study of uncertainties in physical measurements, second., University
680 Science Books, 349 pp., 1997.
- Turner, A. J., Frankenberg, C., and Kort, E. A.: Interpreting contemporary trends in atmospheric methane, *Proc Natl Acad Sci
USA*, 116, 2805–2813, <https://doi.org/10.1073/pnas.1814297116>, 2019.

Yacovitch, T. I., Herndon, S. C., Roscioli, J. R., Floerchinger, C., McGovern, R. M., Agnese, M., Pétron, G., Kofler, J., Sweeney, C., Karion, A., Conley, S. A., Kort, E. A., Nöhle, L., Fischer, M., Hildebrandt, L., Koeth, J., McManus, J. B., Nelson, 685 D. D., Zahniser, M. S., and Kolb, C. E.: Demonstration of an Ethane Spectrometer for Methane Source Identification, *Environ. Sci. Technol.*, 48, 8028–8034, <https://doi.org/10.1021/es501475q>, 2014.

Yacovitch, T. I., Daube, C., and Herndon, S. C.: Methane Emissions from Offshore Oil and Gas Platforms in the Gulf of Mexico, *Environ. Sci. Technol.*, 54, 3530–3538, <https://doi.org/10.1021/acs.est.9b07148>, 2020.

Yang, K., Ting, C., Wang, J., Wingenter, O., and Chan, C.: Diurnal and seasonal cycles of ozone precursors observed from 690 continuous measurement at an urban site in Taiwan, *Atmospheric Environment*, 39, 3221–3230, <https://doi.org/10.1016/j.atmosenv.2005.02.003>, 2005.

Yver-Kwok, C. E., Laurent, O., Guemri, A., Philippon, C., Wastine, B., Rella, C. W., Vuillemin, C., Truong, F., Delmotte, M., Kazan, V., Darding, M., Lebègue, B., Kaiser, C., Xueref-Rémy, I., and Ramonet, M.: Comprehensive laboratory and field testing of cavity ring-down spectroscopy analyzers measuring H₂O, CO₂, CH₄ and CO, *Atmos. Meas. Tech.*, 8, 3867–3892, 695 <https://doi.org/10.5194/amt-8-3867-2015>, 2015.